Available online at www.sciencedirect.com
SCIENCE DIRECT®
Bioorganic & Medicinal Chemistry 13 (2005) 3565–3575
Bioorganic & Medicinal Chemistry

Cytotoxicities, cell cycle and caspase evaluations of 1,6-diaryl-3(*Z*)-hexen-1,5-diynes, 2-(6-aryl-3(*Z*)-hexen-1,5-diynyl)anilines and their derivatives

Chi-Fong Lin,[b] Yu-Hsiang Lo,[a] Ming-Chu Hsieh,[c] Yi-Hua Chen,[a] Jeh-Jeng Wang[a] and Ming-Jung Wu[a,*]

[a]*School of Chemistry, Kaohsiung Medical University, Kaohsiung, Taiwan*
[b]*Department of Biological Science and Technology, Chung Hwa College of Medical Technology, Taiwan, Taiwan*
[c]*Graduate Institute of Pharmaceutical Science, Kaohsiung Medical University, Kaohsiung, Taiwan*

Received 9 December 2004; revised 4 February 2005; accepted 4 February 2005
Available online 30 March 2005

Abstract—Compounds **3**, **6**–**7**, **9**–**10**, **15**–**17**, and **20**–**21** showed growth inhibition effects on a full panel of 60 human cancer cell lines, and most of the average IC_{50} values of the indicated analogues were from <0.01 to 96.6 μM, in which analogues **16** and **17** revealed the highest cytotoxic activity with the cancer cell lines at 10^{-7} M concentration range. During the cell cycle analysis, a moderate to high apoptotic progress induction was shown by **3**, **9**, **16**–**17**, and **20** compared with the control, which 2-(6-(2-thienyl)-3(*Z*)-hexen-1,5-diynyl)aniline **16** showed the highest apoptotic effect. Structures **16**–**17** displayed a significant G2/M phase arrest in the cell growth cycle compared with other derivatives, which the proportions of the G2/M phase cells were accumulated to 71.5% and 82.6%, respectively. Moreover, the colorimetric assay of **16**–**17** also provided advanced evidence to the relationship between the compounds and the caspase-3 enzyme, which was one of the major promoters of apoptotic effect.

1. Introduction

Families of molecules consisting of unique enediyne subdomain cores, which were derived from either natural isolation or synthetic routes, display manifold biological functions.[1,2] Although numerous related studies[1,2] were reported, they only concentrated on the formation of radicals. Except that, there have no investigations describing other feasible physiological active mode, although some biological profiles of such components were explored in our current work.[3] The novel phenomena attracted much of our attention and promoted us to figure out the precise knowledge of the structure–activity relationships (SAR) between cytotoxicities and bioactive mechanisms of these unique structures. It was considered that much more information concerning with these novel enediynes was concealed than it gave, hence, to achieve further significant progress, more studies toward the novel enediynes were necessary to proceed.

In our recent reports, several series of acyclic enediynes, 1-aryl-6-substituted-3(*Z*)-hexen-1,5-diynes **1**,[3a,b] exhibited potent cytotoxic activities with KB, Hela, NCI, DLD, and Hepa cell lines together with the inhibitory activity toward topoisomerase I in low range of micromolar concentrations. It was also found that compounds with an aryl substituent bearing with heteroatoms on C-6 position display higher cytotoxicity than alkyl compounds on that position, in which 2-(6-aryl-3(*Z*)-hexen-1,5-diynyl)benzonitriles **2**[3c] showed G2/M phase arrest and apoptotic effect while the appearance of hetero-atoms (especially the N atom) closed to the C-6 position of enediyne domains. To discover more evidence about the necessity of the N, O hetero-atoms bearing on the C-1 and C-6 positions of the enediyne core with the biological functions presented by these new enediynes, 1,6-diaryl-3(*Z*)-hexen-1,5-diynes **3**–**5**, 1,2-diarylethynyl benzenes **6**–**12**, 2-(6-aryl-3(*Z*)-hexen-1,5-diynyl) anilines **13**–**17** and their derivatives **18**–**22** were designed and synthesized by modification of aryl groups on the C-6 position of the enediyne core. Besides the above compounds, bis-enediynes **23** was also generated to probe the effect of increasing the enediyne cores. These analogues were evaluated for cytotoxic responses

Keywords: Antitumor agents; Enediyne; Caspase; G2/M blocker.
* Corresponding author. Tel.: +886 7 312 1101x2220; fax: +886 7 312 5339; e-mail: mijuwu@cc.kmu.edu.tw

0968-0896/$ - see front matter © 2005 Elsevier Ltd. All rights reserved.
doi:10.1016/j.bmc.2005.02.062

against 60 human tumor cell lines,[4] and the performance of the cell cycle analysis was given to provide advanced insight view of cytotoxicities.

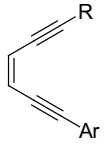

1

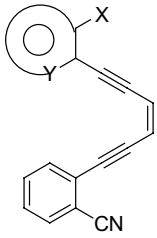

2 (X = N, or O or Y = N)

2. Results

2.1. Chemistry

The synthesis of 1,6-diaryl-3(*Z*)-hexen-1,5-diynes **3**–**5**, and 1,2-diarylethynyl benzenes **6**–**12** was carried out by using *cis*-1,2-dichlorethene **37** or 1,2-diiodobenzene **39** as the starting materials (Scheme 1). Coupling **37** and **39** with trimethylsilylacetylene **28** to give intermediates **38**[5] (70%) and **43**. Compound **38** coupled with aryl iodides **40a**–**c** in the presence of palladium, potassium carbonate in MeOH (method A), to provide **3**–**5** in 35–61% yields. On the other hand, desilylation of **43** with potassium carbonate in methanol produced compound **44** in 86% yield. Then, coupling **44** with various aryl iodides **40a**–**g** by using $Pd(PPh_3)_4$ as a catalyst (method B) gave products **6**–**12** in 30–86% yields, respectively.

Generation of 2-(6-aryl-3(*Z*)-hexen-1,5-diynyl)anilines **13**–**17** and 2-(2-(2-arylethynylphenyl)ethynyl)anilines **18**–**22** was initiated from the coupling reaction between iodoaniline (**27**) and trimethylsilylacetylene (**28**) to give intermediate **29** with the palladium catalyst. Desilylation of **29** with K_2CO_3 in methanol produced compound **30**[6a–c] in 90% yield. Subsequently, Sonogashira coupling reaction[7] of **30** with halides **31**–**32** provided **33** (68%) and **34** (58%), respectively. Palladium-catalyzed coupling reaction (method A) of **33** and **34** with various aryl iodides **40b**–**e** and **40g** gave **13**–**22** in 50–90% yields. The results were summarized in Scheme 2.

1,4-Bis(2-(3(*Z*)-hexen-1,5-diynyl)anilinyl)benzene **23** was accomplished under the same Pd-catalyzed coupling reactions (method A) of **32** with diiodide **41** in 45% yields (Scheme 3).

2.2. Cytotoxicity

Compounds **3**–**5**, **6**–**12**, **13**–**22**, and **23** were submitted to the National Cancer Institute for testing against a panel of approximately 60 tumor cell lines. Details of this test system have been published by others.[8] Derivatives **4**–**5**, **8**, **11**–**14**, **18**–**19**, and **22**–**23** were inactive.[9] The available IC_{50} values of active compounds **3**, **6**–**7**, **9**–**10**, **15**–**17**, and **20**–**21** were from <0.01 to 96.6 μM (data not shown). Obviously, the active compounds displayed a broad-spectrum inhibition on the growth of all 60 cancer cell lines, and most of the average IC_{50} values of **3**, **6**–**7**, **9**–**10**, **15**–**17**, and **20**–**21** were from 10^{-8} to 10^{-6} M. Among the 10 active compounds, 2-(6-(2-thienyl)-3(*Z*)-hexen-1,5-diynyl)aniline **16** and 2-(6-(2-thienyl)-3(*Z*)-hexen-1,5-diynyl)aniline **17** showed the highest cytotoxic activity against some of the full panel

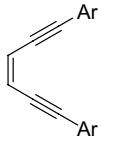

3. Ar = 2-anilinyl
4.Ar = 2-pyridinyl
5.Ar = 2-anisyl

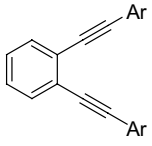

6. Ar = 2-anilinyl
7. Ar = 2-pyridinyl
8. Ar = 2-anisyl
9. Ar = 2-pyrazinyl
10. Ar = 2-thienyl
11. Ar = 4-trifluoromethylphenyl
12. Ar = 2-thioanisyl

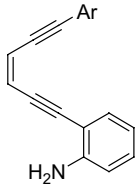

13. 2-pyridinyl
14.2-anisyl
15.2-pyrazinyl
16.2-thienyl
17.2-thieanisyl

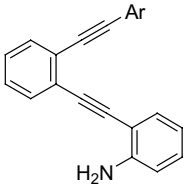

18. 2-pyridinyl
19.2-anisyl
20.2-pyrazinyl
21.2-thienyl
22.2-thieanisyl

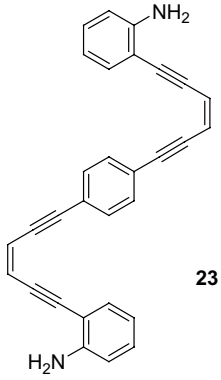

23

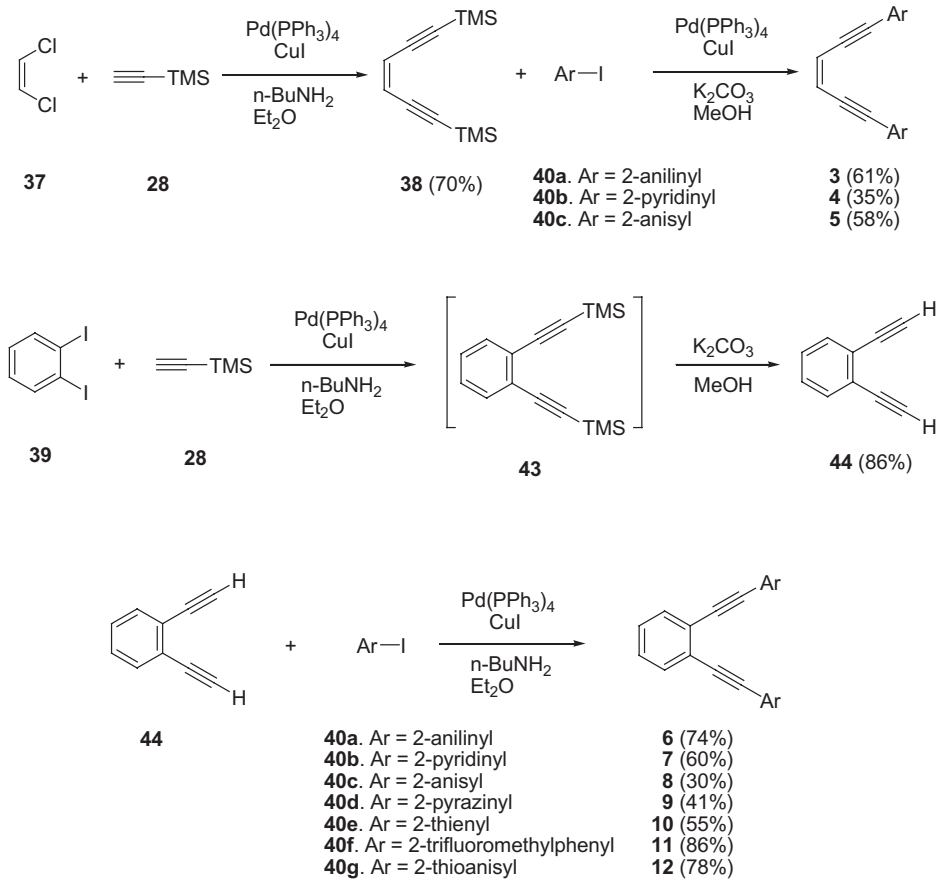

Scheme 1. The synthesis of 1,6-diaryl-3(*Z*)-hexen-1,5-diynes **3**–**5** and 1,2-diarylethynylbenzenes **6**–**12**.

of the 60 tumor cell lines at low 10^{-7} M concentration, especially the IC_{50} value of **16** against the MDA-MB-231/ACTT cell line of human breast cancer was found to be less than 10^{-8} M. It was noted that most of the LC_{50} values of **3**, **6**–**7**, **9**–**10**, **15**–**17**, and **20**–**21** for the 60 cancer cell lines were higher than 10^{-4} M.

2.3. Cell cycle analysis of compounds 3, 6–7, 9–10, 15–17, and 20–21

To obtain much more insight regarding the variances of the enediyne in affecting whole cells, human leukemia K-562 cell was used, and the growth characteristics of cells following treatment with adriamycin, compounds **3**, **6**–**7**, **9**–**10**, **15**–**17**, and **20**–**21** were measured (Figs. 1 and 2). As shown in Figures 1 and 2 (Fig. 1 exchanged to Figs. 3 and 4, Fig. 2 to Figs. 5 and 6), cancer cells were exposed to the vehicle solvent (DMSO) as control, and 50 μM of adriamycin alone with the above derivatives were added to the cell line, in which adriamycin was also used as comparative standard. After exposure to the compounds for 72 h, attached cells were analyzed by flow cytometry. The majority of control cells of the two tests exposed to DMSO and adriamycin were in either the G0/G1 phase (39.5%, 36.6%) or S phase (34.8%, 48.8%) of the cell cycle, and only a few cells in the G2/M phase were detected (25.7%, 14.6%) (Figs. 1 and 2). After treatment with compounds **16** and **17** for 72 h, cells progressed to the G2/M phase, and the majority of the cell population was arrested at the G2/M phase. Consistent with this cell cycle, only 27.5% and 7.6% of the cells were found at the G0/G1 phase, and 0% and 10.0% in S phase, with 71.5% and 82.6% in G2/M phase (Fig. 2).

Compounds **3**, **6**, **7**, **15**, **20**, and **21** showed moderate accumulation of G2/M phase cells, which were 26.9%, 25.2%, 25.1%, 35.4%, 31.4% and 46.5%, respectively. However, remarkable blockage of the K-562 cell cycle in the G2/M phase was observed and induced at the concentration (50 μM) of compounds **16** and **17**. On the other hand, compounds **3**, **6**–**7**, **9**–**10**, **16**–**17**, and **20**–**21** induced moderate to high apoptotic effects of K-562 cells at a concentration of 50 μM. The percentages of apoptosis for **3**, **6**–**7**, **9**–**10**, **16**–**17**, and **20**–**21** and their respective control were as following: **3** (31.3%), **6** (25.5%), **7** (25.2%), **9** (39.4%), **10** (25.1%), and the control (6.70%) (Fig. 4); **16** (15.5%), **17** (11.3%), **20** (8.3%), **21** (7.8%), and their control (6.70%) (Fig. 6). Component **16** revealed the highest induction of apoptosis (15.5%; almost four times than the control) after treating K-562 cells with the compound for 72 h. However, **16** did not show the highest G2/M phase blockage activity for the K-562 cell line.

2.4. Caspase-3 colorimetric assay of compounds 16–17

Besides the examination of influence of the above components toward the cell growth cycle, it was also considered to figure out what factors led the tumor cells into

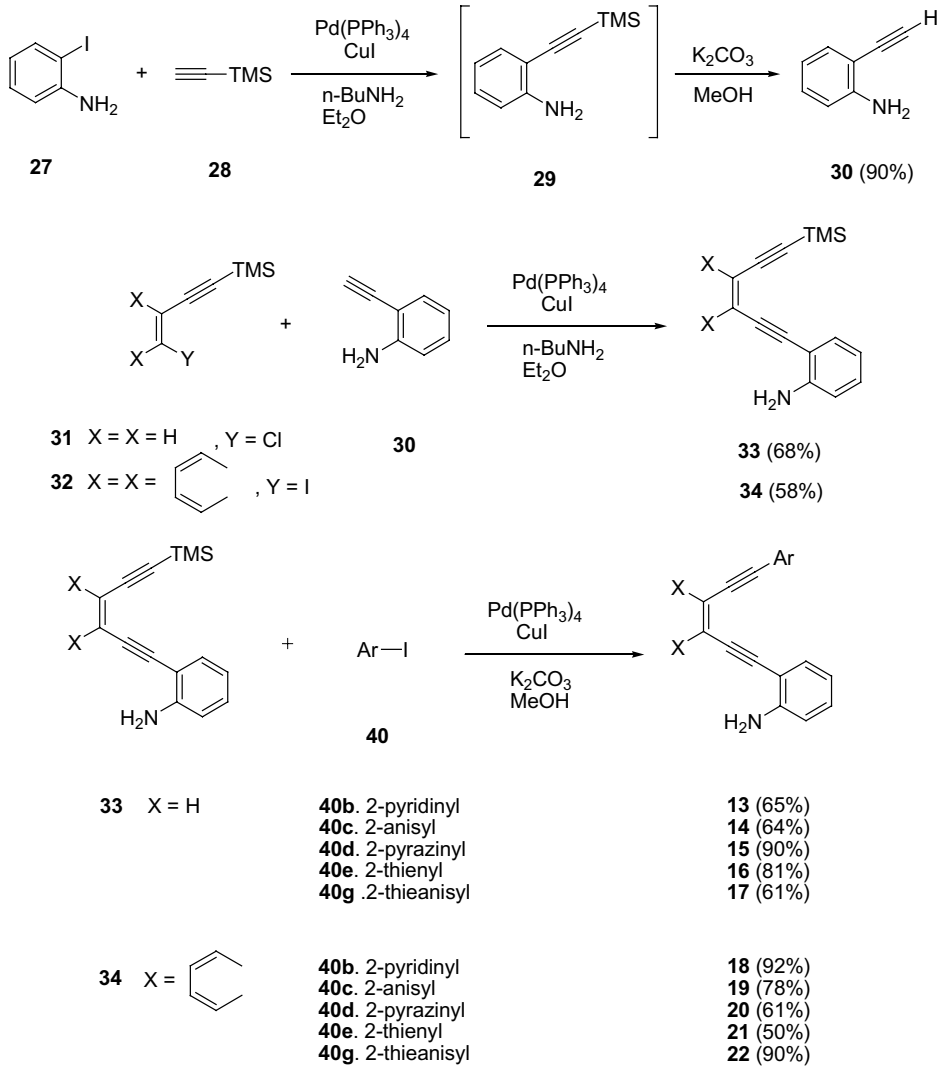

Scheme 2. Generation of 2-(6-aryl-3(*Z*)-hexen-1,5-diynyl)anilines **13**–**17** and 2-(2-(2-arylethynylphenyl)ethynyl)anilines **18**–**22**.

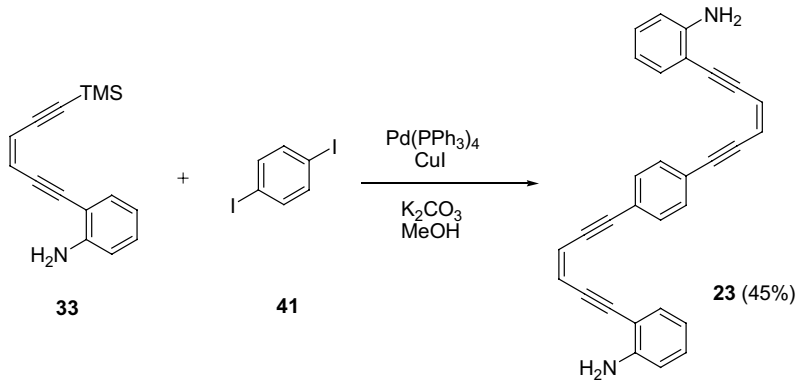

Scheme 3. The synthesis of 1,4-(bis(2-(3(*Z*)-hexen-1,5-diynyl))anilinyl)benzene **23**.

the apoptotic progression; hence, compounds **16** and **17** were treated with the caspase-3, which was the key enzyme correlated with apoptosis induction, and quantified by spectrophotometry at a wavelength of 405 nm. The absorptance of control, DMSO, **16** and **17** were as following: 0.75, 0.99, 1.30 and 1.82, respectively (Fig. 7). Based upon the results, preliminarily, it was demonstrated that the activity of caspase-3 was enhanced by the G2/M blockers **16**–**17** for 1.73 and 2.43 times than control.

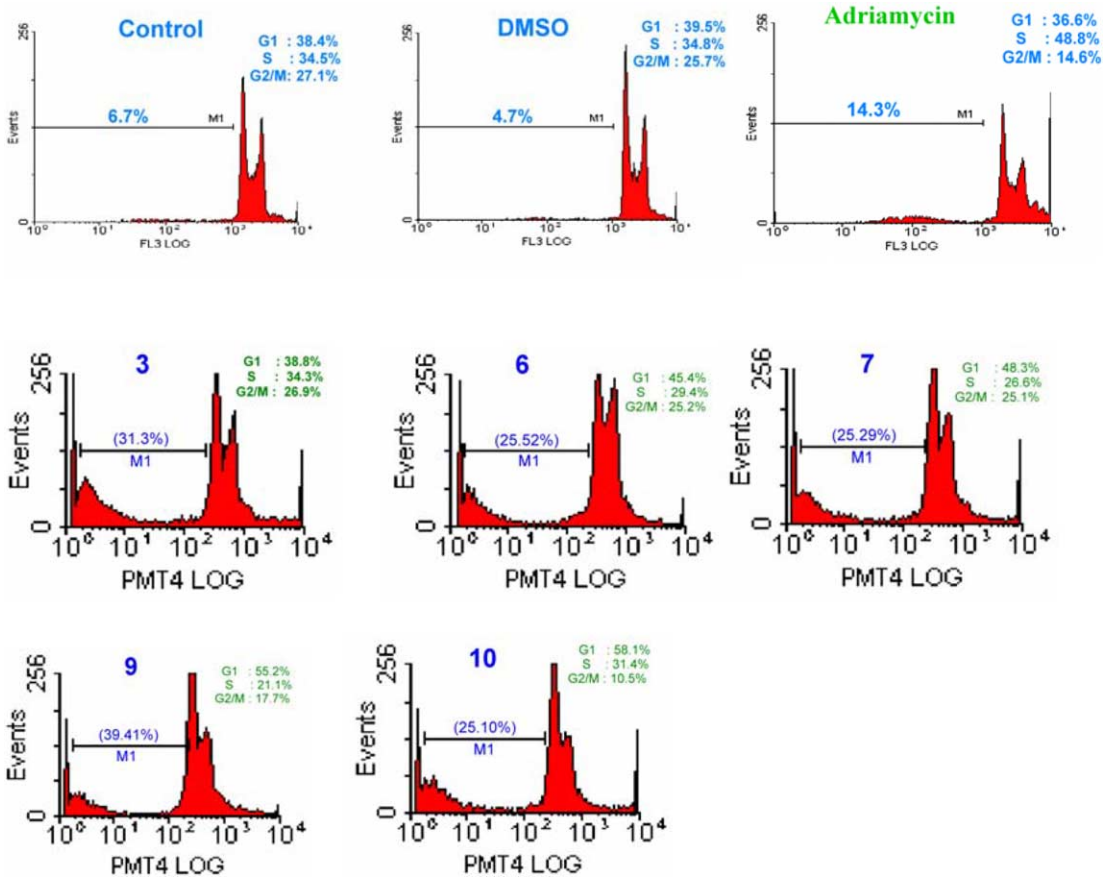

Figure 1. Cell cycle distribution of K-562 cells treated with **3**, **6**–**7**, **9**–**10**, and adriamycin for 72 h used at a concentration of 50 μM by flow cytometry analysis. M1 = apoptotic sub-G1 area.

3. Discussion

To compare with our previous work,[3c] several significant points aroused from this study and the conclusions were summarized in three parts. (1) For the cytotoxic assay: first of all, compounds **3**, **6**–**7**, **9**–**10**, **15**–**17**, and **20**–**21** displayed greater growth inhibitory activities compared with other analogues. It was considered that the essential factors for showing the inhibitory activities on human cancer cells were either containing the N, S atoms in the aryl ring, or bearing NH_2 or SCH_3 groups closed to the C-1 and C-6 positions of the enediyne cores, which probably provided a specific bonding (perhaps covalent or hydrogen bonding) or coordination with metal ions cooperating with the central enediyne. The above prediction could be observed from the weaker cytotoxicity provided by compound **10**, which did not contain the N atom but only bearing the S atom in the structure, though the results were different from those of 2-(6-aryl-3(*Z*)-hexen-1,5-diynyl)benzonitriles **2**. Compound **17** offered the highest cytotoxicity suggested that the substitutions of both anilinyl and thieanisyl subdomains on the enediyne core at the same time existed stronger binding with the unknown target than other derivatives. Secondly, most of all the demonstrated LC_{50} values of compounds **3**, **6**–**7**, **9**–**10**, **15**–**17**, and **20**–**21** for the 60 cancer cell lines were higher than 100 μM, which suggested that the above analogues displayed growth inhibitory activities to human tumor cells, and caused neither normal nor cancer cells' deaths even when the concentrations of these drugs were as high as 100 μM. This phenomenon was unusual and meaningful to the advancement of medical therapies of human cancer diseases, whereas drugs with higher cytotoxic activities always followed the higher damage to normal cells (lower LC_{50} values) and the same properties of components were also demonstrated in the series of 2-(6-aryl-3(*Z*)-hexen-1,5-diynyl)benzonitriles **2**.[3c] (2) For cell cycle assay, according to the data shown in Figures 3 and 5, it was demonstrated that an accumulation of G2/M stage cells in the **16** and **17** samples, when K-562 cells were treated with compounds **3**, **6**–**7**, **9**–**10**, **15**–**17**, and **20**–**21** for 72 h. The percentages of cells at the G2/M phase increased from 16.2% to 71.5% and 82.5% after treatment of K-562 cells with **16** and **17**. Compounds **3**, **6**, **7**, **15**, **20**, and **21** also induced similar G2/M phase blockages. It was noted that all of the active analogues, beside **10**, displayed a better G2/M arrest than adriamycin. It was predicted that G2/M phase arrest was possible due to the inhibition of enzymes essential for G2/M progression or mitosis, especially the tubulin polymerization or depolymerization. (3) On the other hand, almost all active structures (except **15**) led the K-562 cells to apoptotic states at 50 μM, and the effects of apoptotic induction were from 1.5 to 4 times than the control. The apoptotic inductive effects of compounds **3**, **6**–**7**, **9**–**10**, **16**–**17**, and **20**–**21** were better than the derivative **2**. The presentation of apoptotic effect excluded the tumor necrotic factors

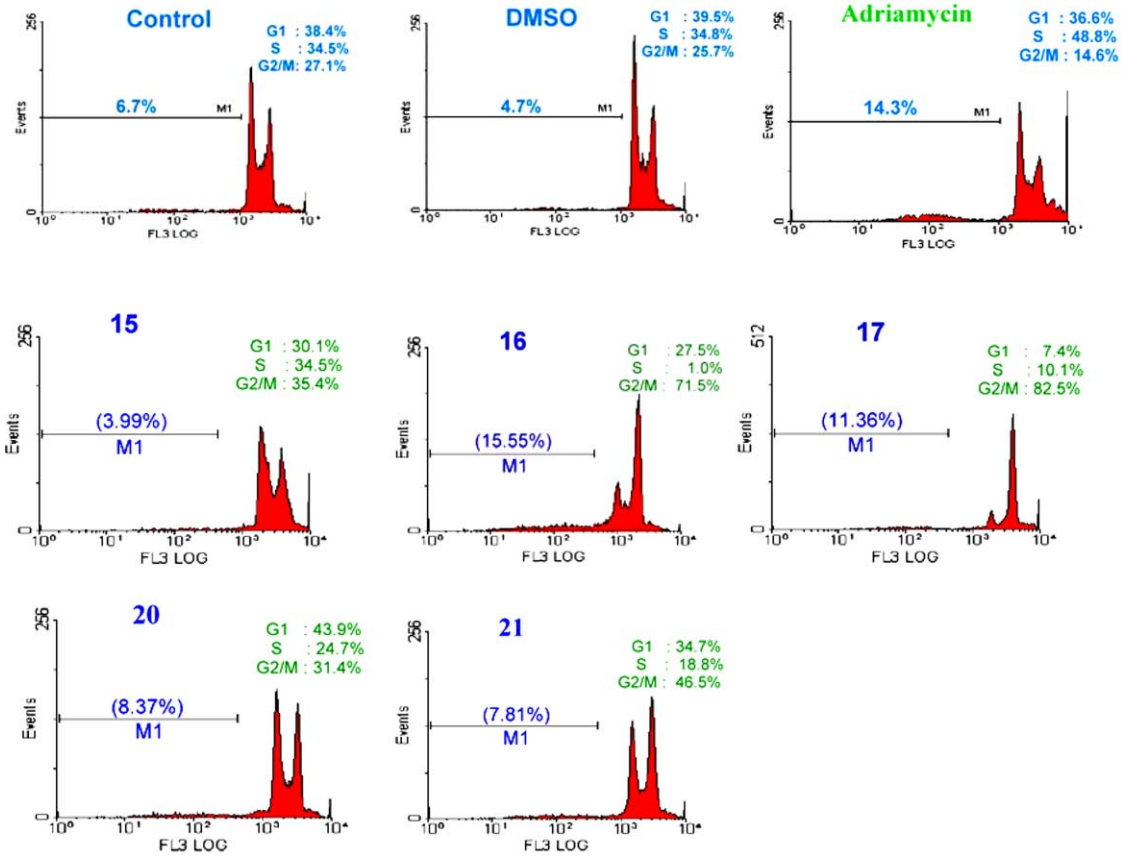

Figure 2. Cell cycle distribution of K-562 cells treated with **15**–**17**, **20**–**21**, and adriamycin for 72 h used at a concentration of 50 μM by flow cytometry analysis. M1 = apoptotic sub-G1 area.

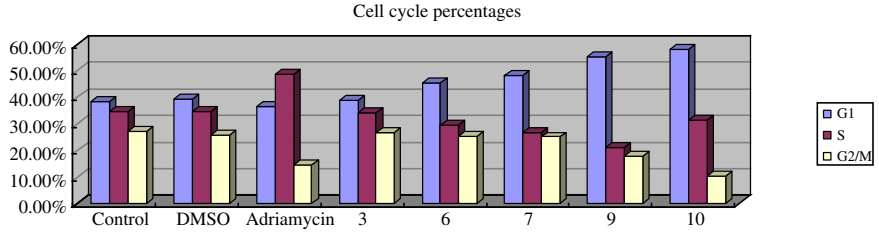

Figure 3. Cell cycle distribution of K-562 cells after treating with compound **3**, **6**–**7**, **9**–**10**, DMSO, and adriamycin. The percentages of the cells in each phase were calculated by using the WinMDI software for the flow cytometry. The percentages of accumulation of G2/M phase cells of the control, adriamycin, and compounds **3**, **6**–**7**, **9**–**10** were 27.1%, 14.6%, 26.9%, 25.2%, 25.1%, 17.7%, and 10.5%, respectively.

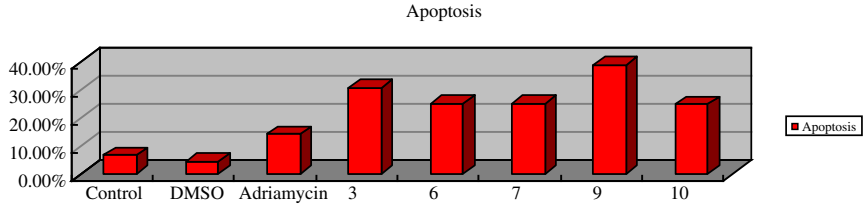

Figure 4. Apoptotic effect induced by adriamycin, compounds **3**, **6**–**7**, and **9**–**10**. The percentages of the cells apoptosis were calculated by using the WinMDI software for the flow cytometry. The proportions of apoptotic cells for compounds **3**, **6**–**7**, **9**–**10**, adriamycin, and the control were: **3** (31.3%), **6** (25.5%), **7** (25.2%), **9** (39.4%), **10** (25.1%), adriamycin (14.3%), and the control (6.7%).

(TNF) for providing cytotoxicities to cancer cells in the presence of **3**, **6**–**7**, **9**–**10**, **16**–**17**, and **20**–**21**. A major part of the phenomenon could be mediated by deregulation in cell cycle progression governed by the families of caspases, especially the caspase-3, which was the straight promoter of apoptosis. The colorimetric assay of capase-3 provided advanced evidence to the relationship between the compounds and the caspase-3 enzyme, though

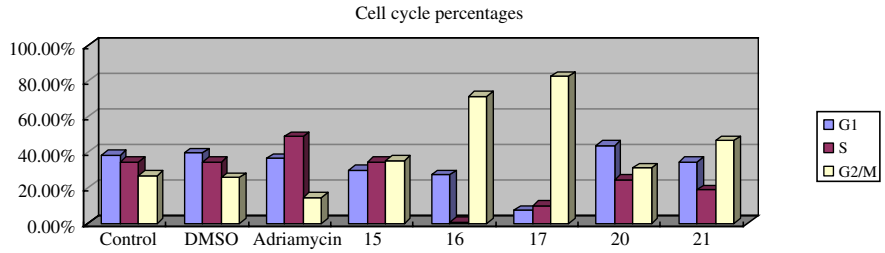

Figure 5. Cell cycle distribution of K-562 cells after treating with compound **15**–**17**, **20**–**21**, DMSO, and adriamycin. The percentages of the cells in each phase were calculated by using the WinMDI software for the flow cytometry. The percentages of accumulation of G2/M phase cells of the control, adriamycin, and compounds **15**–**17**, **20**–**21** were 27.1%, 14.6%, 35.4%, 71.5%, 82.5%, 31.4%, and 46.5%, respectively.

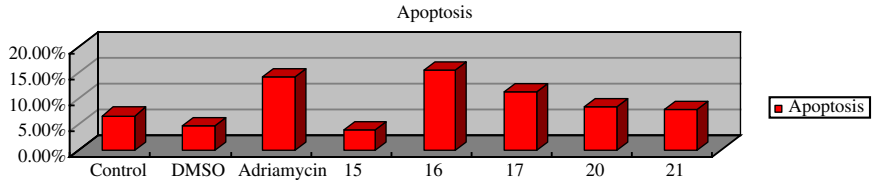

Figure 6. Apoptotic effect induced by adriamycin, compounds **15**–**17** and **20**–**21**. The percentages of the cells apoptosis were calculated by using the WinMDI software for the flow cytometry. The proportions of apoptotic cells for compounds **15**–**17**, **21**–**22**, adriamycin, and the control were: **15** (3.99%), **16** (15.50%), **17** (11.30%), **20** (8.37%), **21** (7.81%), adriamycin (14.3%), and the control (6.7%).

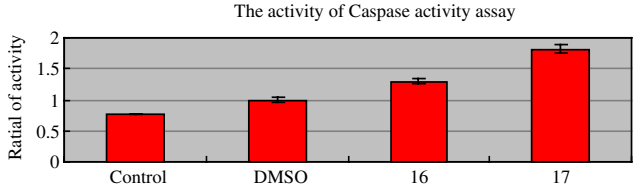

Figure 7. The caspase-3 colorimetric assay of compounds **16**–**17**. The increased enzymatic activities of the caspase-3 in apoptotic were determined by colorimetric reaction. The cleavage of peptide by the caspase releases the chromophore pNA (*p*-nitroaniline), which can be quantified spectrophotometrically at a wavelength of 405 nm. The absorptance for control, DMSO, **16**, and **17** are as following: 0.75(±0.002), 0.99(±0.042), 1.30(±0.037), and 1.82(±0.055). A recombinant caspase-3 enzyme is available for use a positive control (R&D Systems' Catalog # 707-C3).

whether other members of caspases family were enhanced was still unknown and more evidences were necessary for the prediction. However, compounds **3**, **6**–**7**, **9**–**10**, **16**–**17**, and **20**–**21** led K-562 cells to apoptosis,[10] and **16**–**17** displayed a significant G2/M arrest in the cell growth cycle along with the promotion effect with the caspase-3.

4. Conclusions

According to the above results of cytotoxicity, cell cycle assay and the caspase-3 colorimetric assay of compounds **3**–**23**, a clearer picture about the structure–activity relationship was performed (shown in Scheme 4). It was found derivatives **3**, **6**–**7**, **9**–**10**, **15**–**17**, and **20**–**21** showed more potent biological activities than other derivatives during the evaluation course. The profiles were suggested that the biological activities of these compounds were sourced from the appearance of hetero-atoms (N, S) closed to the C-1 and C-6 position of enediyne domains, especially the N atom, and there were no activities revealed with the absence of N, S atoms on those positions. It was thought that the necessity of hetero-atoms (N, S) was probably due to the formation of hydrogen or other essential binding between the hetero-atoms and enediyne core with the target enzymes, especially the presence of N and S atoms bearing on the aryl rings closed to the C-1 and C-6 positions of the enediyne cores together, existed the highest activity, although the results provided by this study gave some differences from that of 2-(6-aryl-3(*Z*)-hexen-1,5-diynyl)benzonitriles **2**. The actual mechanism of **3**, **6**–**7**, **9**–**10**, **15**–**17**, and **20**–**21** was not clear, the inhibitors of essential enzymes of topological and mitosis were considered, especially the enzymes for tubulin polymerization or depolymerization, however, more evidences were necessary to support the assume.

In short, this study has revealed several specific G2/M phase blocker lead compounds together with an apoptotic progress induction via the caspase pathway, and has showed growth inhibition effects on a full panel of 60 human cancer cell lines in low microconcentrations. These new investigations will be helpful in further elucidation of undiscovered biological properties of these novel antitumor enediynes.

5. Experimental

5.1. General procedure for coupling 1,6-bis(trimethylsilyl)3(*Z*)-hexen-1,5-diyne 38 with various aryl iodides (method A)

To a degassed solution of 1,6-bis(trimethylsilyl)3(*Z*)-hexen-1,5-diyne (**38**) (12 mmol) containing CuI (3.2 mmol) and K_2CO_3 (30 mmol) in MeOH (15 mL)

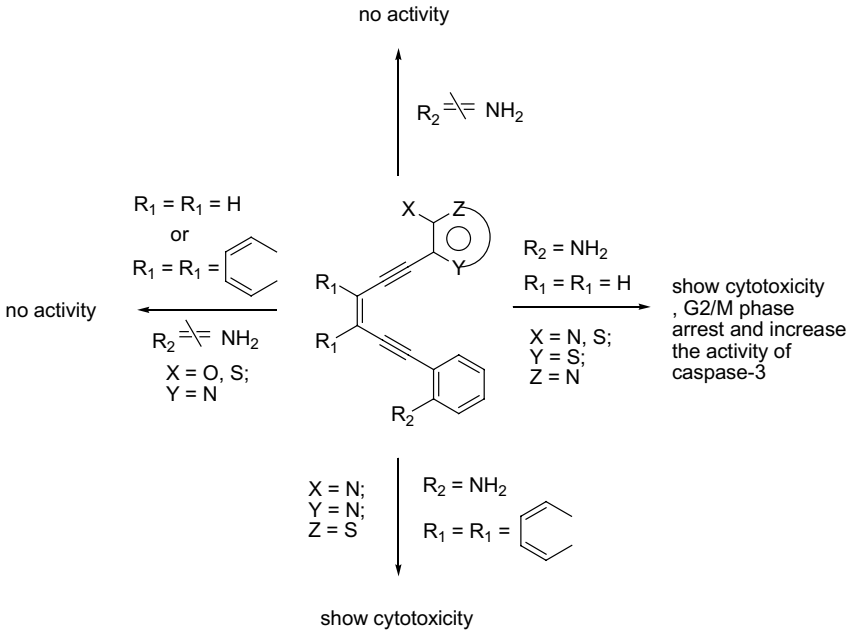

Scheme 4. The preliminary results of the structure–activity relationship (SAR) of 1,6-diaryl-3(*Z*)-hexen-1,5-diynes, 2-(6-aryl-3(*Z*)-hexen-1,5-diynyl)anilines and their derivatives.

was added a degassed solution of aryl iodides (**40a–c**) (12 mmol) containing $Pd(PPh_3)_4$ (0.8 mmol) in MeOH (20 mL). The resulting reaction mixture was stirred for 6 h and removal of methanol in vacuo, and then quenched with saturated aqueous NH_4Cl solution. The aqueous layer was extracted with EtOAc (50 mL) and the combined organic extracts were washed with saturated aqueous Na_2CO_3 solution (40 mL) and dried over anhydrous $MgSO_4$. After filtration and removal of solvent in vacuo, the residue was purified by column chromatography on silica gel to yield the desired products.

5.2. General procedure for coupling 1,2-bis(ethynyl)-benzene 44 with various aryl iodides (method B)

To a degassed solution of 1,2-bis(ethynyl)benzene (**44**) (12 mmol) containing CuI (3.2 mmol) and *n*-$BuNH_2$ (34 mmol) in Et_2O (25 mL) was added a degassed solution of aryl iodides (**40a–g**) (12 mmol) containing $Pd(PPh_3)_4$ (0.8 mmol) in Et_2O (25 mL). The resulting reaction mixture was stirred for 6 h and quenched with saturated aqueous NH_4Cl solution. The aqueous layer was extracted with EtOAc (50 mL) and the combined organic extracts were washed with saturated aqueous Na_2CO_3 solution (40 mL) and dried over anhydrous $MgSO_4$. After filtration and removal of solvent in vacuo, the residue was purified by column chromatography on silica gel to yield the desired products.

5.3. General procedure of the desilylation reaction by using K_2CO_3 in methanol

To a degassed solution of the intermediate 2-(2-trimethylsilylethynyl)aniline **29** (1 mmol) in dry MeOH (10 mL), K_2CO_3 (1.5 mmol) was added to the solution and stirred for 6 h at 25 °C. Then, removal of methanol in vacuo and quenched with saturated aqueous NaCl solutions and extracted with EtOAc. The organic layer was separated and dried over $MgSO_4$. After filtration, the solvent was evaporated in vacuo. The residue was purified by flash chromatography to give the product **30**.

5.4. Cell cycle analysis

Flow cytometry was used to measure cell cycle profile and apoptosis. For cell cycle analysis, K-562 cells treated with compounds **3**, **6–7**, **9–10**, **15–17**, and **20–21** (50 μM) for 24 h were harvested by centrifugation. After being washed with PBS, the cell were fixed with ice-cold 70% ethanol for 30 min, washed with PBS, and then treated with 1 mL of 1 mg/ml of RNase A solution at 37 °C for 30 min. The cells were harvested by centrifugation at 1000 rpm for 5 min and further stained with 250 μL of DNA staining solution (10 mg of propidium iodide [PI], 0.1 mg of trisodium citrate, and 0.03 mL of Triton X-100 were dissolved in 100 mL H_2O) at room temperature for 30 min in the dark. After loading 500 μL of PBS, the DNA contents of 10,000 events were measured by FACScan (Elite ESP, Beckman Coulter, Brea, CA) and the cell cycle profile was analyzed from the DNA content histograms with WinCycle software. When cells were apoptotic the containing DNA were digested by endonuclease then the sub-G1 pick appear. The percentage in sub-G1 was analyzed by gating on cell cycle dot blots using Windows Multiple Document Interface software (WinMDI).

5.5. Caspase-3 colorimetric assay

Human/Mouse Active Caspase-3 assay was conducted for detection of apoptosis in leukemia cell line (K-562). The commercially available apoptosis detection system (R&D systems, MN) was used. K-562 cells treated with compounds **16** and **17** for 48 h were collected by

centrifugation, washed once with PBS, and cell pellets were counted and resuspended in 25 μL/1×10^6 cells of cold Lysis Buffer and homogenized. Homogenates were centrifuged at 12,000 rpm for 10 min at 4 °C, supernatants were used for measuring caspase activity using an ELISA-based assay, according to the manufacturer's instructions.

5.6. 1,2-Diethynylbenzene (44)

^{1}H NMR ($CDCl_3$, 400 MHz) δ 7.52 (dd, 2H, J = 6.0, 3.2 Hz), 7.31 (dd, 2H, J = 6.0, 3.2 Hz), 3.34 (s, 2H); ^{13}C NMR ($CDCl_3$, 100 MHz) δ 132.6, 128.5, 125.0, 81.8, 81.1: MS (EI) [m/z (relative intensity)] 126 (M^+, 100), 73 (10); HRMS calcd for $C_{10}H_6$, M_r = 126.0470, found 126.0461.

5.7. 1,6-Bis (2-anilinyl)-3(*Z*)-hexen-1,5-diyne (3)

^{1}H NMR ($CDCl_3$, 200 MHz) δ 7.34 (dd, 2H, J = 7.6, 1.2 Hz), 7.15 (td, 2H, J = 8.4, 1.8 Hz), 6.75–6.65 (m, 4H), 6.15 (s, 2H), 4.28 (br s, 4H); ^{13}C NMR ($CDCl_3$, 50 MHz) δ 148.1, 132.0, 130.1, 118.3, 117.5, 114.1, 107.1, 94.1, 93.0; MS (EI) [m/z (relative intensity)] 258 (M^+, 100), 257 (92), 256 (74), 255 (21); HRMS calcd for $C_{18}H_{14}N_2$, M_r = 258.1157, found 258.1150.

5.8. 1,6-Dipyrindinyl-3(*Z*)-hexen-1,5-diyne (4)

^{1}H NMR ($CDCl_3$, 200 MHz) δ 8.60 (ddd, 2H, J = 4.8, 2.6, 1.4 Hz), 7.70–7.54 (m, 4H), 7.22 (dt, 2H, J = 7.6, 1.2 Hz), 6.20 (s, 2H); ^{13}C NMR ($CDCl_3$, 50 MHz) δ 150.0, 143.0, 136.0, 127.6, 123.0, 120.4, 96.8, 86.4; MS (EI) [m/z (relative intensity)] 230 (M^+, 100), 229 (59); HRMS calcd for $C_{16}H_{10}N_2$, M_r = 230.0844, found 230.0840.

5.9. 1,6-Bis(2-anisolyl)-3(*Z*)-hexen-1,5-diyne (5)

^{1}H NMR ($CDCl_3$, 200 MHz) 7.51 (dd, 2H, J = 7.7, 2.0 Hz), 7.30 (td, 2H, J = 7.6, 1.8 Hz), 6.95–6.86 (m, 4H), 6.14 (s, 2H), 3.85 (s, 6H); ^{13}C NMR ($CDCl_3$, 50 MHz) δ 159.9, 134.0, 130.0, 120.4, 119.3, 112.5, 110.7, 93.8, 91.5, 55.8; MS (EI) [m/z (relative intensity)] 288 (M^+, 100), 271 (33), 262 (11), 255 (15) 215 (12); HRMS calcd for $C_{20}H_{16}O_2$, M_r = 288.1150, found 288.1143.

5.10. 1,2-Bis(2-anilinyl)ethynylbenzene (6)

^{1}H NMR ($CDCl_3$, 200 MHz) δ 7.57 (dd, 2H, J = 7.0, 1.2 Hz), 7.41–7.30 (m, 4H), 7.15 (dd, 2H, J = 7.2, 1.4 Hz), 6.71 (td, 4H, J = 7.2, 1.0 Hz), 3.51 (br s, 4H); ^{13}C NMR ($CDCl_3$, 50 MHz) δ 148.2, 132.1, 131.7, 130.0, 127.9, 125.3, 117.6, 114.1, 107.3, 93.8, 90.0; MS (EI) [m/z (relative intensity)] 308 (M^+, 100), 307 (53), 306 (39), 305 (15); HRMS calcd for $C_{22}H_{16}N_2$, M_r = 308.1313, found 308.1320.

5.11. 1,2-Bis(2-pyridinyl)ethynylbenzene (7)

^{1}H NMR ($CDCl_3$, 400 MHz) δ 8.65 (dt, 2H, J = 3.1, 1.8 Hz), 7.72–7.64 (m, 6H), 7.40–7.24 (m, 4H); ^{13}C NMR ($CDCl_3$, 100 MHz) δ 149.8, 143.2, 136.4, 132.3, 128.8, 127.8, 125.3, 123.0, 92.6, 88.2; MS (EI) [m/z (relative intensity)] 280 (M^+, 100), 279 (56); HRMS calcd for $C_{20}H_{12}N_2$, M_r = 280.1000, found 280.1005.

5.12. 1,2-Bis(2-anisolyl)ethynylbenzene (8)

^{1}H NMR ($CDCl_3$, 200 MHz) δ 7.58 (td, 4H, J = 5.8, 3.2 Hz), 7.34–7.26 (m, 4H), 6.95–6.86 (m, 4H), 3.81 (s, 6H); ^{13}C NMR ($CDCl_3$, 50 MHz) δ 159.9, 133.9, 131.8, 129.7, 127.6, 126.0, 120.3, 112.6, 110.6, 92.3, 89.9, 55.7; MS (EI) [m/z (relative intensity)] 338 (M^+, 100), 321 (22), 308 (25), 305 (15) 231 (22); HRMS calcd for $C_{24}H_{18}O_2$, M_r = 338.1307, found 338.1319.

5.13. 1,2-Bis(2-pyrazinyl)ethynylbenzene (9)

^{1}H NMR ($CDCl_3$, 200 MHz) δ 8.92 (d, 2H, J = 1.0 Hz), 8.62 (dd, 2H, J = 2.2, 1.6 Hz), 8.51 (d, 2H, J = 1.8 Hz), 7.69 (dd, 2H, J = 6.0, 3.4 Hz), 7.44 (dd, 2H, J = 6.0, 3.4 Hz); ^{13}C NMR ($CDCl_3$, 50 MHz) δ 148.0, 144.5, 143.0, 140.1, 132.3, 129.3, 124.8, 91.2, 90.3; MS (EI) [m/z (relative intensity)] 282 (M^+, 100), 281 (18), 256 (21), 228 (11), 202 (12), 176 (19), 175 (16); HRMS calcd for $C_{18}H_{10}N_4$, M_r = 282.0905, found 282.0912.

5.14. 1,2-Bis(2-thienyl)ethynylbenzene (10)

^{1}H NMR ($CDCl_3$, 400 MHz) δ 7.53 (dd, 2H, J = 11.6, 6.8 Hz), 7.36–7.28 (m, 6H), 7.03 (dd, 2H, J = 10.4, 7.2 Hz); ^{13}C NMR ($CDCl_3$, 100 MHz) δ 132.2, 131.4, 128.0, 127.6, 127.2, 125.3, 123.2, 91.8, 87.0; MS (EI) [m/z (relative intensity)] 290 (M^+, 100), 258 (14), 245 (27), 161 (13), 122 (11), 112 (10); HRMS calcd for $C_{18}H_{10}S_2$, M_r = 290.0224, found 290.0215.

5.15. 1,2-Bis(4-trifluoromethylphenyl)ethynylbenzene (11)

^{1}H NMR ($CDCl_3$, 200 MHz) δ 7.63 (s, 8H), 7.61–7.58 (m, 2H), 7.40–7.35 (m, 2H); ^{13}C NMR ($CDCl_3$, 50 MHz) δ 132.1, 131.8, 131.6, 130.6, 128.7, 126.9, 125.5, 125.4, 92.2, 90.3; MS (EI) [m/z (relative intensity)] 414 (M^+, 100), 395 (9), 344 (10), 276 (9), 28 (25); HRMS calcd for $C_{24}H_{12}F_6$, M_r = 414.0843, found 414.0839.

5.16. 1,2-Bis(2-thieanisolyl)ethynylbenzene (12)

^{1}H NMR ($CDCl_3$, 200 MHz) δ 7.63 (dd, 2H, J = 5.8, 3.6 Hz), 7.56 (dd, 2H, J = 5.8, 1.4 Hz), 7.32 (dd, 2H, J = 5.8, 3.2 Hz), 7.19–7.15 (m, 2H), 7.09 (td, 2H, J = 7.4, 1.4 Hz), 2.48 (s, 6H); ^{13}C NMR ($CDCl_3$, 50 MHz) δ 141.9, 132.8, 132.2, 128.7, 128.0, 125.2, 124.2, 121.9, 94.6, 91.1, 15.3; MS (EI) [m/z (relative intensity)] 349 (M^+, 55), 340 (19), 338 (13), 228 (14), 221 (100); HRMS calcd for $C_{24}H_{18}S_2$, M_r = 370.0850, found 370.0806.

5.17. 2-(6-(2-Pyridinyl)-3(*Z*)-hexen-1,5-diynyl)aniline (13)

^{1}H NMR ($CDCl_3$, 200 MHz) δ 8.59 (d, 1H, J = 4.4 Hz), 7.63 (td, 1H, J = 7.6, 1.8 Hz), 7.46 (d, 1H, J = 7.6 Hz),

7.30 (dd, 1H, J = 7.6, 1.4 Hz), 7.24–7.07 (m, 2H), 6.71–6.61 (m, 2H), 6.26 (d, 1H, J = 11.0 Hz), 6.06 (d, 1H, J = 10.6 Hz), 4.39 (br s, 2H); ^{13}C NMR ($CDCl_3$, 50 MHz) δ 149.9, 148.7, 142.9, 136.0, 131.8, 130.3, 127.5, 122.8, 121.5, 117.3, 116.7, 114.0, 106.8, 95.7, 95.6, 93.0, 87.4; MS (EI) [m/z (relative intensity)] 244 (M^+, 100), 243 (91), 241 (24); HRMS calcd for $C_{17}H_{12}N_2$, M_r = 244.1001, found 244.0995.

5.18. 2-(6-(2-Anisolyl)-3(*Z*)-hexen-1,5-diynyl)aniline (14)

^{1}H NMR ($CDCl_3$, 200 MHz) δ 7.47 (dd, 1H, J = 7.4, 1.6 Hz), 7.36–7.28 (m, 2H), 7.13 (td, 1H, J = 7.4, 1.6 Hz), 6.96 (d, 1H, J = 8.0 Hz), 6.89 (d, 1H, J = 8.0 Hz), 6.72–6.64 (m, 2H), 6.15 (m, 2H), 4.41 (br s, 2H), 3.85 (s,3H); ^{13}C NMR ($CDCl_3$, 50 MHz) δ 159.9, 148.3, 133.8, 130.1, 130.0, 120.4, 119.0, 118.4, 117.4, 114.0, 112.2, 110.8, 107.4, 94.3, 93.6, 93.2, 91.7, 55.6; MS (EI) [m/z (relative intensity)] 273 (M^+, 85), 272 (52), 257 (100), 254 (25), 231 (36), 168 (40); HRMS calcd for $C_{19}H_{15}ON$, M_r = 273.1154, found 273.1126.

5.19. 2-(6-(2-Pyrazinyl)-3(*Z*)-hexen-1,5-diynyl)aniline (15)

^{1}H NMR ($CDCl_3$, 200 MHz) δ 8.71 (d, 1H, J = 1.6 Hz), 8.55 (t, 1H, J = 2.6 Hz), 8.46 (d, 1H, J = 2.4 Hz), 7.30 (d, 1H, J = 2.0 Hz), 7.13 (td, 1H, J = 8.0, 1.4 Hz), 6.72–6.63 (m, 2H), 6.31 (d, 1H, J = 11.0 Hz), 6.07 (d, 1H, J = 11.0 Hz), 4.21 (br s, 2H); ^{13}C NMR ($CDCl_3$, 50 MHz) δ 148.7, 147.9, 144.5, 142.8, 140.0, 132.0, 130.6, 122.9, 117.6, 115.9, 114.2, 106.7, 96.5, 92.8, 92.7, 91.4; MS (EI) [m/z (relative intensity)] 245 (M^+, 100), 244 (76), 192 (52), 191 (75), 190 (35), 164 (33); HRMS calcd for $C_{16}H_{11}N_3$, M_r = 245.0954, found 245.0964.

5.20. 2-(6-(2-Thienyl)-3(*Z*)-hexen-1,5-diynyl)aniline (16)

^{1}H NMR ($CDCl_3$, 200 MHz) δ 7.36 (dd, 1H, J = 5.4, 1.8 Hz), 7.33 (dd, 1H, J = 2.6, 1.2 Hz), 7.29 (dd, 1H, J = 3.8, 1.2 Hz), 7.03 (dd, 1H, J = 5.2, 3.6 Hz), 6.74–6.08 (m, 2H), 6.18 (d, 1H, J = 10.6 Hz), 6.09 (d, 1H, J = 10.6 Hz), 4.35 (br s, 2H); ^{13}C NMR ($CDCl_3$, 50 MHz) δ 148.3, 132.7, 131.9, 130.2, 128.0, 127.2, 122.9, 119.4, 117.6, 117.5, 114.1, 107.2, 94.9, 93.2, 91.8, 90.2; MS (EI) [m/z (relative intensity)] 249 (M^+, 100), 247 (27), 246 (38), 208 (34); HRMS calcd for $C_{16}H_{11}NS$, M_r = 249.0613, found 249.0594.

5.21. 2-(6-(2-Thieanisolyl)-3(*Z*)-hexen-1,5-diynyl)aniline (17)

^{1}H NMR ($CDCl_3$, 200 MHz) δ 7.45 (dd, 1H, J = 7.6, 1.4 Hz), 7.36–7.25 (m, 2H) 7.17–7.05 (m, 3H), 6.71–6.63 (m, 2H), 6.17 (m, 2H), 2.42 (s, 3H); ^{13}C NMR ($CDCl_3$, 50 MHz) δ 148.2, 141.8, 132.7, 132.1, 130.0, 129.0, 124.3, 124.2, 121.1, 119.5, 117.8, 117.5, 114.0, 107.4, 94.6, 94.4, 93.8, 93.0, 15.0; MS (EI) [m/z (relative intensity)] 289 (M^+, 72), 274 (86), 273 (100), 272 (24); HRMS calcd for $C_{19}H_{15}NS$, M_r = 289.0926, found 289.0921.

5.22. (1-(2-Anilinylethynyl)-2-(2-pyridinylethynyl))-benzene (18)

^{1}H NMR ($CDCl_3$, 200 MHz) δ 8.60 (dd, 1H, J = 4.0, 0.8 Hz), 7.67–7.52 (m, 4H), 7.43–7.07 (m, 5H), 6.71–6.64 (m, 2H), 4.41 (br s, 2H); ^{13}C NMR ($CDCl_3$, 50 MHz) δ 149.8, 148.4, 143.2, 135.9, 132.4, 131.9, 131.3, 129.8, 128.6, 127.5, 127.5, 126.3, 123.9, 122.7, 117.3, 114.1, 107.3, 93.3, 92.2, 91.0, 88.4; MS (EI) [m/z (relative intensity)] 249 (M^+, 100), 291 (35); HRMS calcd for $C_{21}H_{14}N_2$, M_r = 294.1157, found 294.1127.

5.23. (1-(2-Anilinylethynyl)-2-(2-anisolylethynyl))benzene (19)

^{1}H NMR ($CDCl_3$, 200 MHz) δ 7.56–7.52 (m, 3H), 7.41 (dd, 1H, J = 7.8, 1.6 Hz), 7.38–7.28 (m, 3H), 6.99–6.87 (m, 2H), 6.73–6.64 (m, 2H), 4.01 (br s, 2H), 3.83 (s, 3H); ^{13}C NMR ($CDCl_3$, 50 MHz) 160.1, 148.3, 133.8, 132.1, 132.0, 131.4, 130.0, 129.7, 127.9, 127.6, 125.8, 125.5, 120.4, 117.4, 113.9, 112.4, 110.8, 107.7, 93.7, 92.7, 90.4, 89.6, 55.8; MS (EI) [m/z (relative intensity)] 323 (M^+, 100), 308 (23), 307 (31), 279 (28), 217 (21), 205 (20); HRMS calcd for $C_{23}H_{17}ON$, M_r = 323.1310, found 323.1310.

5.24. (1-(2-Anilinylethynyl)-2-(2-pyrazinylethynyl))-benzene (20)

^{1}H NMR ($CDCl_3$, 200 MHz) δ 8.79 (d, 1H, J = 1.4 Hz), 8.56 (dd, 1H, J = 2.6, 1.4 Hz), 8.47 (d, 1H, J = 2.6 Hz), 7.67–7.59 (m, 2H), 7.57–7.28 (m, 3H), 6.73–6.65 (m, 2H), 4.26 (br s, 2H); ^{13}C NMR ($CDCl_3$, 50 MHz) δ 148.4, 148.1, 144.3, 142.8, 140.2, 132.6, 132.1, 131.6, 130.1, 129.3, 127.7, 126.6, 123.2, 117.6, 114.3, 107.3, 93.0, 92.5, 91.4, 89.4; MS (EI) [m/z (relative intensity)] 295 (M^+, 61), 294 (35), 247 (11); HRMS calcd for $C_{20}H_{13}N_3$, M_r = 295.1109, found 295.1124.

5.25. (1-(2-Anilinylethynyl)-2-(2-thienylethynyl))benzene (21)

^{1}H NMR ($CDCl_3$, 200 MHz) δ 7.60–7.53 (m, 2H), 7.44 (dd, 1H, J = 8.4, 1.8 Hz), 7.38–7.30 (m, 3H), 7.16 (td, 1H, J = 7.8, 1.6 Hz), 7.04 (dd, 1H, J = 4.6, 3.6 Hz), 6.75–6.68 (m, 2H), 4.12 (br s, 2H); ^{13}C NMR ($CDCl_3$, 50 MHz) δ 148.1, 132.6, 131.9, 131.3, 129.9, 128.3, 127.7, 127.1, 125.6, 124.5, 122.8, 117.5, 114.0, 107.4, 93.5, 92.4, 90.6, 86.2; MS (EI) [m/z (relative intensity)] 299 (M^+, 100), 298 (36), 297 (35), 265 (14), 216 (13), 214 (15), 149 (16); HRMS calcd for $C_{20}H_{13}NS$, M_r = 299.0762, found 299.0777.

5.26. (1-(2-Anilinylethynyl)-2-(2-thieanisolylethynyl))-benzene (22)

^{1}H NMR ($CDCl_3$, 200 MHz) δ 7.69–7.51 (m, 3H), 7.45–7.28 (m, 4H), 7.20–7.07 (m, 3H), 6.70–6.65 (m, 2H), 4.12 (br s, 2H), 2.44 (s, 3H); ^{13}C NMR ($CDCl_3$, 50 MHz) δ 148.2, 142.1, 132.6, 132.3, 132.1, 131.5, 129.7, 128.9, 128.2, 127.6, 125.6, 125.1, 124.3, 124.2, 123.2, 117.5, 114.0, 107.8, 94.9, 93.6, 90.6, 90.5, 15.1; MS (EI) [m/z (relative intensity)] 339 (M^+, 55), 325 (25), 324 (87),

323 (100); HRMS calcd for $C_{23}H_{17}NS$, M_r = 339.1082, found 339.1063.

5.27. 1,4-Bis(6-(2-anilinyl)-3(*Z*)-hexen-1,5-diynyl)-benzene (23)

^{1}H NMR ($CDCl_3$, 200 MHz) δ 7.48 (s, 2H), 7.33 (dd, 1H, J = 8.0, 1.4 Hz), 7.15 (td, 1H, J = 7.6, 1.4 Hz),6.74–6.68 (m, 2H), 6.21 (d, 1H, J = 11.0 Hz), 6.09 (d, 1H, J = 11.0 Hz), 3.87 (br s, 2H); ^{13}C NMR ($CDCl_3$, 50 MHz) δ 147.9, 132.0, 131.8, 130.3, 123.1, 120.1, 118.0, 117.7, 114.4, 107.5, 97.2, 96.5, 94.9, 93.2, 90.0; MS (EI) [*m*/*z* (relative intensity)] 408 (M^+, 100), 407 (21), 406 (19), 405 (10), 241 (11); HRMS calcd for $C_{30}H_{20}N_2$, M_r = 408.1628, found 408.1591.

Acknowledgements

We would like to thank the National Science Council of the Republic of China and National Institutes of Health (National Cancer Institute) for their financial support.

References and notes

1. (a) Jones, G. B.; Hynd, G.; Wright, J. M.; Purohit, A.; Plourde, G. W.; Huber, R. S.; Mathews, J. E.; Li, A.; Kilgore, M. W.; Bubley, G. J.; Yancisin, M.; Brown, M. A. *J. Org. Chem.* **2001**, *66*, 3688; (b) Alabugin, I. V.; Manoharan, M.; Kovalenko, S. V. *Org. Lett.* **2002**, *4*, 1119; (c) Walkers, S.; Valentine, K. G.; Kahne, D. *J. Am. Chem. Soc.* **1990**, *112*, 6428; (d) Dark, L.; Iwasawa, N.; Danishefsky, S.; Crother, D. M. *Proc. Natl. Acad. Sci. U.S.A.* **1991**, *88*, 7464; (e) Povirk, L. F.; Goldberg, I. H. *Biochemistry* **1980**, *19*, 4773; (f) Myers, A. G.; Kuo, E. Y.; Finny, N. S. *J. Am. Chem. Soc.* **1989**, *111*, 8057; (g) Kappen, L. S.; Goldberg, I. H. *Nucleic Acid Res.* **1978**, *5*, 2959.
2. (a) Jones, G. B.; Wright, J. M.; Hynd, G.; Wyatt, J. K.; Yancisin, M.; Brown, M. A. *Org. Lett.* **2000**, *2*, 1863; (b) Wu, M. J.; Lin, C. F.; Chen, S. H.; Lee, F. C. *J. Chem. Soc., Perkin Trans. 1* **1999**, 2875; (c) Wendi, D. M.; Kerwin, S. M. *J. Am. Chem. Soc.* **1997**, *119*, 1464; (d) Tarli, A.; Wang, K. K. *J. Org. Chem.* **1997**, *62*, 8841; (e) Lin, C. F.; Wu, M. J. *J. Org. Chem.* **1997**, *62*, 4546; (f) Wu, M. J.; Lin, C. F.; Ong, C. W. *Bioorg. Med. Chem. Lett.* **1996**, *6*, 675; (g) Wu, M. J.; Lin, C. F.; Wu, J. S.; Chen, H. T. *Tetrahedron Lett.* **1994**, *35*, 1879; (h) Xu, S. L.; Moore, H. W. *J. Org. Chem.* **1992**, *57*, 326; (i) Myers, A. G. *Tetrahedron Lett.* **1987**, *28*, 4493; (j) Lockhart, T. P.; Comita, P. B.; Bergman, R. G. *J. Am. Chem. Soc.* **1981**, *103*, 4082; (k) Jones, R. R.; Bergman, R. G. *J. Am. Chem. Soc.* **1972**, *94*, 660; (l) Bergman, R. G. *Acc. Chem. Res.* **1973**, *6*, 25.
3. (a) Lin, C. F.; Lu, W. D.; Hsieh, P. C.; Kuo, Y. H.; Wang, C. J.; Wu, M. J. *Helv. Chim. Acta* **2002**, *8*, 2564; (b) Lin, C. F.; Hsieh, P. C.; Lu, W. D.; Chiu, H. F.; Wu, M. J. *Bioorg. Med. Chem.* **2001**, *9*, 1707; (c) Lo, Y. H.; Lin, C. F.; Hsieh, M. C.; Wu, M. J. *Bioorg. Med. Chem.* **2004**, *12*, 1047.
4. The cytotoxic evaluations of compounds **3**–**23** were supported by National Cancer Institute.
5. (a) Herunsalee, A.; Isobe, M.; Goto, T. *Tetrahedron* **1991**, *23*, 3727; (b) McMahon, R. J.; Halter, R. J.; Fimmen, R. L.; Wilson, R. J.; Peebles, S. A.; Kuczkowski, R. L.; Stanton, J. F. *J. Am. Chem. Soc.* **2000**, *5*, 939; (c) Walker, J. A.; Bitler, S. P.; Wudl, F. *J. Org. Chem.* **1984**, *24*, 4733; (d) Tsukiyama, T.; Isobe, M. *Tetrahedron Lett.* **1992**, *51*, 7911; (e) McPhee, M. M.; Kerwin, S. M. *J. Org. Chem.* **1996**, *26*, 9385.
6. (a) Bosch, E.; Jeffries, L. *Tetrahedron Lett.* **2001**, *46*, 8141; (b) Arcadi, A.; Cacchi, S.; Marinelli, F. *Tetrahedron Lett.* **1989**, *19*, 2581; (c) Simth, K. L.; Ray, P. S. *Heterocycles* **1997**, *1*, 11.
7. Sonogashira, K.; Yatake, T.; Tohda, Y.; Takahashi, S.; Hagihara, N. *Chem. Commun.* **1977**, 291.
8. (a) Boyd, M. R. Status of implementation of the NCI human tumor cell in vitro primary drug screen. *Am. Assoc. Cancer Res.* **1989**, *30*, 652; (b) Monks, A.; Scudiero, D.; Skehan, P.; Shoemaker, R.; Poull, K.; Vistica, D.; Hose, C.; Langley, J.; Cronise, P.; Vaigro-Wolff, A.; Gray-Goodrich, M.; Cambell, H.; Mayo, J.; Boyd, M. *J. Natl. Cancer Inst.* **1991**, *83*, 757.
9. The primary anticancer assays of compounds **3**–**23** were tested for three tumor cell lines consisting of the MCF7 (breast cancer), NCI-H460 (non-small cell lung cancer), and SF-268 (CNS cancer). Compounds **3**, **6**–**7**, **9**–**10**, **15**–**17**, and **20**–**21**, which reduced the growth of any one of the cell lines to approximately 32% or less were passed on for evaluation in the full panel of 60 cell lines.
10. (a) Wajant, H.; Pfizenmaier, K.; Scheurich, P. *Cell Death Differen.* **2003**, *10*, 45; (b) Martin, B.; Kirsty, M.; Chan, S. W.; Luzio, J. P.; Robert, S.; Weissberg, P. *Science* **1998**, *282*, 290.